



저작자표시-비영리-변경금지 2.0 대한민국

이용자는 아래의 조건을 따르는 경우에 한하여 자유롭게

- 이 저작물을 복제, 배포, 전송, 전시, 공연 및 방송할 수 있습니다.

다음과 같은 조건을 따라야 합니다:



저작자표시. 귀하는 원저작자를 표시하여야 합니다.



비영리. 귀하는 이 저작물을 영리 목적으로 이용할 수 없습니다.



변경금지. 귀하는 이 저작물을 개작, 변형 또는 가공할 수 없습니다.

- 귀하는, 이 저작물의 재이용이나 배포의 경우, 이 저작물에 적용된 이용허락조건을 명확하게 나타내어야 합니다.
- 저작권자로부터 별도의 허가를 받으면 이러한 조건들은 적용되지 않습니다.

저작권법에 따른 이용자의 권리는 위의 내용에 의하여 영향을 받지 않습니다.

이것은 [이용허락규약\(Legal Code\)](#)을 이해하기 쉽게 요약한 것입니다.

[Disclaimer](#)

Master's Thesis

Directional control of angiogenesis to produce a
designed multiscale micro-vascular network with
bioprinting

Sung Joon Hong

Department of Biomedical Engineering

Graduate School of UNIST

2018

Directional control of angiogenesis to produce a
designed multiscale micro-vascular network with
bioprinting

Sung Joon Hong

Department of Biomedical Engineering

Graduate School of UNIST

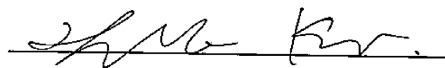
Directional control of angiogenesis to produce a
designed multiscale micro-vascular network with
bioprinting

A thesis/dissertation
submitted to the Graduate School of UNIST
in partial fulfillment of the
requirements for the degree of
Master of Science

Sung Joon Hong

07. 09. 2018

Approved by



Advisor

Hyun-Wook Kang

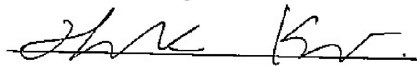
Directional control of angiogenesis to produce a
designed multiscale micro-vascular network with
bioprinting

Sung Joon Hong

This certifies that the thesis/dissertation of Sung Joon Hong is approved.

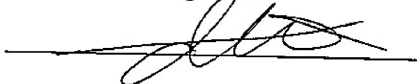
07/09/2018

signature



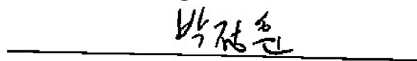
Advisor: Hyun-Wook Kang

signature



Thesis Committee: Woonggyu Jung

signature



Thesis Committee: Chung Hun Park

ABSTRACT

The biomimetic vascular network is a key element in regeneration of viable, functional and scalable artificial tissues. In this study, we developed a multiscale vascular network that can be patterned freely by using bioprinting technology. An endothelialized channel of several hundred micrometer scale was directly printed. The micro-vascular network consisting of tubular structures of several tens of micrometers was generated through the direction control of angiogenic sprouting using the chemotaxis effect. For this purpose, human umbilical vein endothelial cells (HUVEC) and angiogenic factor secreting cells, normal human dermal fibroblasts (NHDF), were co-patterned at 1 to 2 mm intervals using water soluble bio-ink and alginate based bio-ink, respectively. Then, a bridge pattern connecting the two patterned gels was made with fibrin gel. After printing, an endothelialized channel of about 800 μm was formed by selective removal of water soluble bio-ink. The angiogenic sprouting was induced at about 200 $\mu\text{m}/\text{day}$ along the bridge pattern from the channel. It was also possible to fabricate a multiscale micro-vascular network with diagonal, wave and branch shapes using bridge patterns of various designs. In this study, we investigated the functionality of hepatocytes by co-culturing mouse primary hepatocytes after fabricating a vascular construct with hepatic lobule-shaped pattern to confirm the utility of the constructed process. As a result, we could confirm largely improved albumin and urea secretion. Based on these results, we confirmed that the tissue specific multiscale vascular network could be constructed. This technique should provide a useful tool for the development of functional and scalable vascularized tissues.

Key words: 3D bioprinting, microvasculature patterning, angiogenesis, gradient of angiogenic factor,

Contents

1. Introduction	1
2. Material and Methods	2
3D bioprinting system	2
Preparation of Bio-ink and synthetic polymer.....	2
Cell culture and hepatocyte isolation	3
Construction of vascular structure with capillary network.....	3
Fabrication of bio-mimetic liver lobule structure.....	4
Viability analysis	4
Immunostaining.....	5
Connectivity analysis	5
Image analysis.....	5
Simulation of angiogenic factor profile.....	6
Gel compressive modulus test.....	6
Albumin & Urea Secretion quantification.....	6
Statistical analysis	6
3. Results	7
Formation of endothelialized channel and micro-vascular network.	7
Difference in sprouting by concentration of fibrin of surrounding matrix.	7
Construction of designed 3D micro-vascular structure with bioprinting technology.....	7
Micro-vessel network formation via bridge gel patterning	8
Effect of distance on angiogenic sprouting	9
Comparison with angiogenesis and vasculogenesis model	9
Patterning of micro-vascular networks.....	10
Biomimetic liver lobule-shaped vascular network and its functionality	11
4. Discussion.....	11
5. Conclusion.....	13

List of figures

Fig. 1.....	14
Fig. 2.....	14
Fig. 3.....	15
Fig. 4.....	15
Fig. 5.....	16
Fig. 6.....	16
Fig. 7.....	17
Fig. 8.....	17
Fig. 9.....	18
Fig. 10.....	19

1. Introduction

Fabrication technology of biomimetic vascular network is a key component technology for viable, scalable and functional artificial tissue regeneration. Without proper micro-vessels, adequate delivery of oxygen and nutrients and waste removal cannot be achieved due to the limit of mass transfer into tissues, and the function is not maintained for a long time. In addition, each tissue in the body has specific micro-vascular patterns, which greatly affect the microfluidic environment in the tissue. For example, the hepatic lobule unit that constitutes the liver is composed of hepatocytes and hepatic sinusoids and has the form of hexagonal plates. And the liver sinusoidal wave has a micro-vascular network of radial arrangement around the central vein. This vascular pattern directly affects survival and function of the parenchymal cells constituting the tissue. In fact, several studies have reported that in-vivo implantation of an artificial tissue with a specific patterned micro-vascular network improves blood flow and tissue functions[1, 2]. Therefore, the production of biomimetic micro-vascular patterns is a key point for the regeneration and function improvement of the tissue.

Recently, a variety of techniques have been introduced to produce a designed artificial micro-vascular network. A micro-vasculature fabrication technique with a parallel pattern has been introduced using molding technology[3]. And that the flow of blood through the micro-vessel implanted in animal and the functionality of the parenchymal cell are improved. And the study showed that the flow of blood through the grafted micro-vessels and the improved functionality of the parenchymal cells in the construct. However, only micro-vascular networks with parallel patterns have been introduced. In addition, various technologies for patterning micro-vessels using a 3D bio-printing system have been introduced. Techniques were developed to fabricate structures with soluble materials and to generate micro-vessels using them as a mold[1, 2]. A technique for directly patterning the required endothelialized channels using water soluble bio-ink was also introduced [4-7]. However, the vascular network produced by bioprinting has been limited to tubular structures on the scale of hundreds of micrometers. The vascular network in the body is composed of various scales ranging from tens to hundreds of micrometers and has a tissue specific pattern. Although a variety of techniques have been introduced so far, micro-vascular patterning techniques with multi-scales have not yet been introduced.

Here, we have developed a fabrication technique for a multiscale micro-vascular network that can be patterned and constructed of tubular structures on the scale of tens to hundreds of micrometers using 3D bioprinting technology. Endothelialized channels of several hundred micrometers in diameter were made directly by bioprinting. A micro-vascular network consisting of several tens of micro-scale tubular structures was constructed by controlling the direction of angiogenic sprouting. Angiogenesis is induced by angiogenic factors such as VEGF, and the direction of angiogenic sprouting is determined by the concentration gradient of the factor[8, 9]. In this study, we developed a micro-vascular network with parallel, diagonal, wave, and branch shapes from the endothelialized channel through various

experiments. Based on these results, it was confirmed that the designed multiscale micro-vascular network can be fabricated. We also applied our vascular network fabrication technology to liver tissue engineering to confirm the usefulness of the constructed process. A liver lobule-shaped vascular network with a hexagonal plate shape was constructed and then co-cultured with mouse primary hepatocytes. As a result, we confirmed that the vascular network greatly enhanced hepatocyte function in terms of albumin and urea secretion. The key advantage of this technique is the ability to freely control the pattern of a multiscale micro-vascular network of tubular structures ranging from tens to hundreds of micrometers. This technique will provide a crucial tool for artificial regeneration of functional and scalable vascularized tissues.

2. Material and Methods

3D bioprinting system

3D bioprinting system is consist of motorized XYZ stage, multiple cartridges and closed chamber. Three-axis stage system has a working space of 100 x 100 x 100 mm and its resolution of X, Y and z axis are 250 nm, 250 nm and 500 nm respectively. The multiple cartridges have dispensing module to control precisely the volume of synthetic polymers or bio-ink. Quantitative syringe Dispenser (SMP3; Musashi Engineering, Inc.), precision pneumatic pressure controller (ML-808FXcom; Musashi Engineering, Inc., Japan), syringe heater (TCD-200EX; Iwashita Engineering, Inc., Japan), syringe (Normject; Henke Sass Wolf, Germany) and nozzle (Musashi Engineering, Inc.) were used. The closed chamber system has multiple functions of temperature control, UV sterilization, HEPA filtration to optimize the bio-printing process.

Preparation of Bio-ink and synthetic polymer

To produce 3D micro-vascularized structure with 3D bio-printer, we used three different composite hydrogels (gelatin hydrogel, alginate hydrogel, bridge pattern gel) and PCL polymer as supporting material. Briefly, the gelatin hydrogel was made by mixing gelatin, hyaluronic acid(HA) and glycerol. HA (3 mg/ml) was dissolved in Minimum Essential Medium (MEM) by rotating the solution at 37°C overnight. Gelatin (37.5 mg/ml) was added into the solution and gently shaken for 1h. Then glycerol (4% v/v) was added into the solution and shaken for 30 min at 37°C. The other two composite hydrogels are based on the gelatin hydrogel. In case of alginate hydrogel, alginate (1.5% w/v) was added and dissolved in the gelatin hydrogel. The bridge pattern gel has additional component of fibrinogen (2.5 mg/ml) in gelatin hydrogel. Gelatin hydrogel was used as a sacrificial material for vascular channel formation and alginate hydrogel was used to print NHDF. Bridge pattern gel was used for promoting angiogenesis and controlling the pattern of micro-vascular network.

All prepared bio-inks were sterilized by filtration through a 0.45 μm syringe filter and stored at -80°C before use. After the bio-ink was dissolved in a water bath at 37°C, the cells were gently mixed in the bio-ink. Before use, PCL (Mw; 43,000~50,000, Polysciences, Inc.) used as the supporting material was melted at 90°C.

Cell culture and hepatocyte isolation

Primary HUVECs (Lonza) and GFP-HUVECs (Angioproteomie) were cultured in EGM-2 media (EGM-2 bullet kit; Lonza) and passages 4 to 8 used for experiments. NHDF were cultured in FGM-2 (FGM-2 bullet kit; Lonza) and used up to passage 9. Cell cultures were grown to 80% confluence prior to passage or use in experiments. All cells were maintained in a humidified incubator at 37°C and 5% CO₂ and culture media were changed every two days.

All animal studies are conducted according to protocols approved by the UNIST Institutional Animal Care and Use Committee. Primary mouse hepatocytes were isolated from 8-week-old male C57BL/6 mouse. Hepatocytes were isolated using two steps collagenase perfusion method. Viability of the hepatocytes after isolation was confirmed to >85% by Trypan blue exclusion method. After isolation, Isolated hepatocytes were used by mixing with media. The medium used was composed of William's medium E with 10% FBS, 1% L-glutamine, 6 μg / ml aprotinin and 1% penicillin / streptomycin.

Construction of vascular structure with capillary network

Vascular structure was constructed with multi-material applicable 3D bioprinter by layer-by-layer deposition method. Previously described, four components were used for printing three composite hydrogels and polycaprolactone (PCL) as supporting material. Each bio-ink was loaded on 1ml plastic syringe and PCL was loaded on metal syringe. Different size of metal nozzles for each component were used to fabricate desired structure (gelatin hydrogel - 200 μm nozzle, bridge pattern - 100 μm nozzle, alginate hydrogel - 300 μm nozzle, PCL – 300 μm nozzle). During printing process, the inside of the bioprinter chamber was maintained at 18 °C for gelation of gelatin-based bio-inks.

To form the two vascular channels, gelatin hydrogel as a sacrificial material was mixed with HUVEC (10 M/ml) and printed in a linear pattern. NHDFs (20 M/ml) was embedded in alginate hydrogel and patterned with a straight line between two HUVEC-laden gelatin hydrogels. This allowed NHDF to secrete angiogenic factor to inducing sprouting from HUVEC channels during the culture of the construct. NHDF pattern and HUVEC channels were placed at a distance from each other, and the concentration gradient of angiogenic factor was generated in the space. For micro-vascular pattern control, bridge pattern with low concentration fibrinogen concentration was

used to connect HUVEC channel and NHDF pattern. The bridge pattern was printed differently according to the desired micro-vascular pattern. After printing, the structure was quickly covered with fibrin gel (fibrinogen 10 mg/ml, thrombin 2.5 U/ml, CaCl₂ 40 mM) as a surrounding matrix, and incubated for 30 minutes at room temperature for crosslinking. Subsequently, the sample was covered with sufficient EGM-2 media for covering the construct and maintained in a humidified incubator at 37°C and 5% CO₂. The media was changed one day after the production and then changed every two days.

The vasculogenesis model was constructed by inducing vasculogenesis by connecting HUVEC channels with bridge pattern containing HUVEC (1 M/ml) and NHDF (2 M/ml) without NHDF-laden alginate gel. In order to induce both angiogenesis and vasculogenesis in the combined model, NHDF-laden alginate gels were printed between HUVEC channels, and HUVECs were embedded in the bridge pattern.

Fabrication of bio-mimetic liver lobule structure

To demonstrate the functionality of the engineered micro-vascular network, we constructed micro-vascular structures mimicking the hepatic lobule structure of liver tissue. The framework of the structure was formed by PCL and hexagonal blood vessel channels were formed using gelatin hydrogel containing HUVEC (10 M cells/ml). In order to induce angiogenesis at the center of the structure, NHDF-laden alginate gel (20 M cells/ml) was printed in column-shaped form at the height of the structure, and bridge pattern was connected between NHDF-laden alginate gel and HUVEC-laden gelatin gel. After printing, the structure was covered with fibrin gel (fibrinogen 10mg/ml, thrombin 2.5 U/ml, CaCl₂ 40 mM) as a surrounding matrix. After incubation at room temperature for 30 minutes for gelation of the fibrin gel, the printed structure was incubated on EGM-2 media. On the day 5 of culture, alginate lyase (2 U/ml) was added to culture media to dissolve alginate gel and cultured for another 2 days. Then, mouse primary hepatocyte was mixed with hepatocyte media (20 M cells/ml) and 1.5 µl of the mixed solution was seeded in the alginate gel column. After incubation for 30 min at 37 °C, the construct was covered with 10 µl of fibrin gel and incubated with EGM-2 + DMEM + 10% FBS + 1% P/S + Primary Hepatocyte Maintenance Supplements (Thermo scientific, CM4000) for 5 days.

Viability analysis

To determine cell viability within the printed structures, live/dead viability/cytotoxicity kit was used. After washing with PBS, the samples were stained using calcein-AM (“live”; 0.5 µL/ml;

Invitrogen) and ethidium homodimer (“dead”; 2 μ L/ml; Invitrogen) and incubated at room temperature for 1 hour. The images were obtained using a fluorescent microscope (DM2500, Leica). Total four fluorescence images were taken from each sample and the number of live and dead cells were counted manually.

Immunostaining

Samples were fixed with 4% paraformaldehyde (Sigma) for 1 hour and permeabilized with 0.15% triton-X (sigma) 100 for 1 hour at room temperature. To minimize nonspecific binding of antibodies, samples were treated with 3% bovine serum albumin (Sigma) for 1 hour at room temperature. Primary antibodies against CYP450 reductase (1:100; Abcam, cat. no. ab13513, USA), albumin (1:100, Santa cruz, cat. no. sc374670 AF647) were diluted in saline and incubated overnight at 4°C. After washing with saline, the samples were labelled with secondary Alexa568 anti-rabbit antibody (1:1000, Thermo scientific, cat. no. A11036) for 4h at room temperature. For nuclei staining, the samples were incubated with Hoechst 33342 (1:1000, Sigma) for 2h at room temperature. All samples were washed three times between each step and were stored in saline before imaging.

Connectivity analysis

To test the connectivity of induced micro-vessels, we used 1 μ m red fluorescence beads (Polysciences) suspended in PBS solution. After 7 days of culture, samples were fixed with 4% PFA and introduced the diluted solution (1:1000) of fluorescence beads to the entrance of the vascular channel. Then, the samples were incubated for 24h at 4°C to give enough time for the beads to enter through the micro-vessels. Following the incubation, they were imaged using fluorescent microscope.

Image analysis

Fluorescent images were obtained using a fluorescent microscope (DM2500, Leica) or a confocal microscope (FV1000, Olympus). Images were analyzed by Fiji. The length of sprouts was determined by measuring the distance between the edge of HUVEC channel and the tip of each sprout. The number of junctions and vessel widths were measured manually. The orientation of the micro-vessels was analyzed using the directionality plugin (Fiji). Angle 0° was set perpendicular to the HUVEC channel. The vascular area coverage was determined from images of micro-vascular networks obtained at day 1, 5 and 9. To optimize the analysis, the images were converted into two-dimensional binary images by thresholding in according to its original three-dimensional image. Then vascular area coverage was measured by calculating the proportion of the fluorescent pixels within the bridge pattern area (ROI of each image). The images of micro-vascular lumen were obtained using a confocal microscope.

Simulation of angiogenic factor profile

To show the shape of angiogenic factors gradient generated by diffusion in developed micro-vascularized tissue, we performed two-dimensional simulation using a conventional simulation program (ansys workbench 18.2, Ansys Inc.). The diffusion coefficient of angiogenic factors was assumed to be $1.0 \times 10^{-4} \text{ mm}^2/\text{s}$ in the bridge gel and $1.0 \times 10^{-5} \text{ mm}^2/\text{s}$ in fibrin gel[10]. Angiogenic factor secretion rate of NHDF was assumed to be $1.458 \times 10^{-8} \text{ ng/cells/hour}$ [11]. The diffusion of angiogenic factors was simulated by using Fick's second law $(\delta C) / (\delta t) = D (\delta^2 C) / (\delta x^2)$. C is the concentration of angiogenic factors (mol/m^3) and D is the diffusion coefficient (mm^2/s).

Gel compressive modulus test

Compressive modulus of fibrin gel was measured by using Instron 3342 (Instron, Norwood, MA, USA). The compression force was 1 mm/min. The stress-strain curve slope between 5 and 15% strain was measured as a compressive modulus.

Albumin & Urea Secretion quantification

To evaluate the functionality of isolated primary hepatocytes within vascular constructs, albumin and urea secretion were analyzed. As a control group, hepatocyte 3D hydrogel culture was used by embedding the hepatocytes into the fibrin gel at a density of $20 \text{ M}/\text{ml}$. Hepatocyte-fibrin gel mixture was cultured in non-treated 24-well plates ($50 \mu\text{l}$ per well). This fibrin gel was same with the surrounding matrix of the vascular constructs. Culture media from the control and samples were collected on day 1, 3 and 5 after culturing hepatocytes and then stored at -80°C until the assay. The quantification of albumin and urea were determined using mouse albumin assay kit (Komabiotech, cat. no. K3231007) and QuantiChrom™ Urea Assay Kit (Bioassay Systems, cat. no. DIUR-100), respectively, according to the manufacturer's protocol.

Statistical analysis

All data were expressed as means \pm standard deviation (SD) or mean \pm standard error of the mean (SEM). Statistical analyses were performed using GraphPad Prism software (version 5.01; GraphPad, CA, USA). Statistical comparisons between experimental groups were analyzed using Student's t-test or one-way analysis of variance (ANOVA). A value of $P < 0.05$ was considered as statistically significant.

3. Results

Formation of endothelialized channel and micro-vascular network.

To induce micro-vessel formation in micro-vascular construct, we co-printed HUVEC and NHDF. Large blood vessels with diameters of several hundred micrometers were fabricated by patterning HUVEC-embedded gelatin-based hydrogel. Since gelatin is thermo-reversible, when the construct was incubated at 37 °C, gelatin gel melted to form a hollow channel, then HUVEC attached to the channel wall and formed an endothelialized channel.

Fibroblast is one of the major cell types that produces angiogenic factors that induce endothelial cells to cause angiogenesis. Fibroblasts were embedded in alginate-based gels and printed at a distance between the two endothelialized channels. This arrangement lead to the formation of concentration gradient of secreted angiogenic factor in the fibrin matrix, from the fibroblasts to the endothelialized channel (Fig. 1a). The concentration gradient of angiogenic factor is well known to induce angiogenesis and determining the direction of sprouting [8]. The outside of the printed structure was covered with polycaprolactone (Fig. 1b), and the inside of the structure was covered with a surrounding matrix of fibrin gel of 10 mg/ml (Fig. 1c). The printed vascular construct had a size of 7 mm x 5 mm x 1.6 mm.

Difference in sprouting by concentration of fibrin of surrounding matrix.

To determine the appropriate concentration of fibrinogen in the surrounding matrix for micro-vascular construct formation, we prepared samples with different fibrinogen concentrations (2.5, 5 or 10 mg/ml). At 2.5 mg/ml, the sprouts started to stretch one day after the incubation, reaching a length of about 500 μm on day 5 (Fig.2 a-c). Within 5 mg/ml and 10 mg/ml, sprouting started from the third day of cultivation and reached to about 400 μm and 250 μm on the fifth day, respectively (Fig.2 d-i). Also, sprouting occurred more in the direction of NHDF which secretes angiogenic factors than the opposite direction (fig2. J, k). The lower concentration of fibrinogen in the matrix, the faster the angiogenic sprouting occurred and the greater the number of sprouts. However, in the case of gel with low concentration, the matrix degradation rapidly proceeded and the structure could not be maintained for a long time. In case of 2.5 mg/ml gel, the structure melted after 7 days of incubation, but in 10 mg/ml gel, the construct could be maintained and cultured for more than 2 weeks.

Construction of designed 3D micro-vascular structure with bioprinting technology

We placed the bridge pattern between HUVEC channel and NHDF pattern with low concentrations of fibrinogen (2.5 mg/ml) to stimulate sprouting in the endothelialized channel and to regulate the pattern of micro-vascular formation. High concentration (10 mg/ml) fibrin gel was used as the surrounding

matrix for structural maintenance and long-term culture. Because Bridge gel contain low concentration of fibrinogen than fibrin matrix and weak mechanical properties, it promoted angiogenic sprouting from HUVEC channel in bridge pattern. In addition, diffusion of the angiogenic factors secreted by the NHDF formed a concentration gradient in the bridge pattern over time (Fig. 3a). For this reason, we hypothesized that pattern control of micro-vessels could be possible by controlling the pattern of bridge gels.

The printed vascular structures were successfully fabricated in the desired pattern and had a size of 10 mm x 6.5 mm x 1.6 mm (Fig. 3b). Next, we measured cell viability inside the printed structure. Immediately after printing, HUVECs of endothelialized channel and NHDFs embedded in alginate gel had 92% and 93% viability, respectively. Both cells maintained high viability over 90% until 7 days cultivation (Fig. 4).

Micro-vessel network formation via bridge gel patterning

After bioprinting, the formation of micro-vasculature on the scale of several tens of micrometers was observed through the cell culture process. HUVEC channel and NHDF pattern were arranged at 1 mm intervals, and samples with a parallel bridge pattern were prepared (Fig. 5a). From the third day of culture, angiogenic sprouting was induced along the bridge pattern from the endothelialized channel toward the NHDF pattern. The induction of sprouting was continued for 7 days (Fig. 5b). Microvasculature was generated only in the bridge pattern and not in the surrounding matrix. In this study, the angiogenic sprouting was induced only in the bridge pattern by giving the stiffness difference between the bridge pattern and the surrounding matrix. As a result of measuring the compressive modulus of the two materials, the modulus of the surrounding matrix showed about 3 times higher than that of the bridge pattern (Fig. 5c). This result is consistent with previous studies which showed the angiogenesis is more likely to occur when the matrix's mechanical property is low[10, 12, 13]. On day 9, micro-vasculature generated from both HUVEC channels were connected to each other though the NHDF pattern. Induced micro-vessels had a lumen with a diameter of about 30 μm was confirmed using confocal microscopy (Fig. 5e). In addition, 1 μm diameter fluorescent micro-beads were injected into the endothelialized channel and the beads partially flowed into the induced micro-vessels (Fig. 5f). Micro-beads that pass completely through the micro-vascular network were not observed for repeated experiments. Taken together, these results showed that co-patterning of endothelial cells and growth factor secreting cells can be used to fabricate large vascular and tubular micro-vascular networks with a diameter of several tens of micrometers.

Effect of distance on angiogenic sprouting

The effect of distance between endothelial cell and fibroblast pattern on angiogenic sprouting was examined. For this purpose, the structures were constructed with four groups with spacing of 1, 2, 3, and 4 mm. The morphology of the induced micro-vessels was observed for 9 days cultivation after printing (Fig. 6). The 1, 2 mm group showed that angiogenic sprouting was induced along the bridge pattern and formed an intricate micro-vascular network. However, sprouting in 3 and 4 mm groups did not form micro-vascular network properly and showed a similar morphology to cell migration. Based on these results, it was found that endothelial cells and fibroblasts placed at more than a certain distance did not induce proper angiogenic sprouting.

Quantitative analysis of one and two millimeter distance groups was performed by measuring the sprouts lengths and numbers of junctions of the induced micro-vessels. On day 5, most of the micro-vessels formed in the 1 mm group extended to the end of the bridge gel pattern. When the micro-vessels reached to the alginate hydrogel, it showed slower rate of angiogenic sprouting. In the 2 mm group, the sprouts extended to 1800 μm on day 9 (Fig 7a). There was no significant difference in sprouting speed between the two groups considering the length of the bridge gel. Both groups showed similar extending rates of about 200 $\mu\text{m}/\text{day}$. In both groups, the number of vessel junctions increased with the passage of time, indicating that an intricate vascular network was formed (Fig 7b). There was no significant difference in the number of junctions between the two groups. These results show that the distance between the endothelial cell and the fibroblast does not have a significant effect on the speed of angiogenic sprouting and junction formation unless the distance exceeds certain value.

Comparison with angiogenesis and vasculogenesis model

In previous studies, strategies for producing in vitro micro-vascular network are largely divided into angiogenesis[14-17] and vasculogenesis[18-21]. In this study, the previously developed angiogenesis model (Fig. 8a) was compared with other models. For this purpose, vasculogenesis models (Fig. 8b) and combined models (Fig. 8c) were prepared. In the vasculogenesis model, bridge pattern connecting two endothelialized channels were produced using HUVEC and NHDF laden ink, without printing NHDF-laden alginate gel. The combined model combines fabrication method of the two models described above. This model allows the simultaneous induction of angiogenesis and vasculogenesis printing endothelialized channel, NHDFs pattern and bridge pattern with two cells. After constructing and culturing the three models, morphology of endothelial cells within bridge pattern in each of the three groups was observed by fluorescence microscopy. In the angiogenesis model, a bundle of linear vascular structures was formed from the endothelialized channel toward the fibroblast pattern as shown in the previous section (Fig. 8a). In the vasculogenesis model, however, simultaneous vasculogenesis occurred in every part of the bridge pattern. Angiogenic sprouting from the endothelialized channel was

not observed, and connection with the resulting micro-vascular network and the channel was not observed (Fig. 8b-i). In the combined model, the observed phenomena in both models occurred simultaneously. The fastest formation of the micro-vascular network among the three groups was observed and induced micro-vessels showed connectivity with endothelialized channels (Fig. 8c-i and 8c-ii). In all groups, micro-vascular networks were formed only in the bridge pattern and not in the surrounding matrix.

For the quantitative analysis of the micro-vascular network generated in each model, we examined its directionality, vessel width and vessel area coverage (Fig. 8d-h). Directionality is a measure of alignment of the vessels in the direction of the bridge pattern (Fig. 8d-f). The micro-vessels of the angiogenesis model showed the most aligned directionality in the bridge pattern direction. Based on the angle of the bridge pattern of $\pm 18^\circ$, the micro-vessels of the angiogenesis model showed about 1.5 times better alignment than the combined model and about 1.8 times better than the vasculogenesis model. Among the three groups, the vasculogenesis model showed the most random orientation. The angiogenesis model showed the largest vessel width of about 20 μm (Fig. 8g). The combined model showed a vessel width of about 16 μm , slightly larger than the vasculogenesis model, but no statistical significance was observed. On the other hand, the combined model showed the best results in terms of speed of micro-vessels formation (Fig. 8h). Until 5 days in culture, the combined model showed the fastest vessel area coverage. The combined model and angiogenesis model showed similar coverage on day 9. Vasculogenesis model showed only a coverage of about 25% on day 9. These results show that angiogenesis model has somewhat slower vessel formation rate than combined model but has better directionality and similar coverage on day 9 of culture. Based on these results, an angiogenesis model was used for further studies to induce micro-vascular networks with specific patterns.

Patterning of micro-vascular networks

Based on the angiogenesis model with excellent alignment, we examined whether the micro-vascular network pattern can be controlled. For this, two bridge patterns with diagonal and wave shapes were prepared (Fig. 9a, b). As a result, it was confirmed that angiogenic sprouting was performed depending on the shape of the bridge pattern. In the diagonal pattern, a vascular network was formed at an angle of 45° (Fig. 9a-i, ii). In the bridge pattern with the wave shape, it was observed that the arranged vascular network was formed (Fig. 9b-i, ii). Through two experiments, it was confirmed that the direction of angiogenic sprouting can be controlled by controlling the bridge pattern.

Based on these results, we attempted to fabricate vascular constructs with a more complex and biomimetic branch pattern. To induce this complex pattern of micro-vessel network, a bridge pattern with a branch shape that was split twice was made (Fig. 9c and Fig. 3b). Angiogenic sprouting was

formed along the designed branch pattern during 13 days of culture. For detailed analysis, angiogenic factor gradient along the pathway of the bridge pattern was examined using computer simulation technology (Fig. 9d, e). Simulation results showed that concentration gradient of fibroblast-secreted factors was formed within the bridge pattern that the NHDF pattern side had higher concentration and the HUVEC channel side had lower (Fig. 9d, e, black line). Also, this gradient was well formed at the second branch of the branch pattern (Fig. 9d, e, blue line). These data indicate that the direction of angiogenic sprouting is highly correlated with chemotaxis formed by concentration gradient of angiogenic factors.

Biomimetic liver lobule-shaped vascular network and its functionality

Liver lobule-shaped structure using mouse primary hepatocyte was constructed by our patterning strategy of multiscale vascular network (Fig. 10a, b) and its functionality was measured. HUVEC channels with hexagonal shape was fabricated by direct patterning (Fig. 10a, b, c). In order to induce angiogenic sprouting, NHDFs were placed in the center and a bridge pattern with a radial pattern was formed. As shown in the previous results, angiogenic sprouting was radially induced along the bridge pattern during culturing (Fig. 10d, e). After micro-vascular network was formed in the middle position, fibroblast-laden alginate gel was removed using alginate lyase on day 9 of culture (Fig. 10f, g). Then, the isolated mouse primary hepatocytes were manually placed in the center (Fig. 10h). After three days of hepatocyte seeding, albumin and CYP450 reductase staining showed the hepatocyte function and metabolic activity were maintained (Fig. 10i, j). The amount of albumin and urea secreted from the hepatocytes of the printed construct was measured using a medium sampled on 4 day of culture and compared with a group without a vascular network (3D fibrin gel control). The hepatocyte cultured with the multiscale vascular network showed an albumin secretion that was about 3 times higher than the control group (Fig. 10k) and 40 times higher urea secretion. These results indicate that the induced micro-vascular network greatly enhanced hepatocyte function.

4. Discussion

So far, various researchers have attempted to make artificial vascular using bioprinting technology. A number of techniques to produce endothelialized channels of several hundred micrometers in diameter have been introduced as well as large vessels such as artery [22-28]. Also, It has been reported that the viability and functionality of the artificial tissue can be greatly improved using these techniques [22, 23, 25]. The micro-vascular networks in the body exist in various scale. Blood vessels with a diameter of hundreds to tens of micrometers are arranged very closely and have a specific pattern. Although various studies have been introduced so far, the structure control technique of a multiscale vascular network,

which has blood vessels of several hundreds and tens of micrometers in diameter, has not yet been developed. This is because of the resolution limit of bioprinting technology, it is only possible to manufacture vascular channel with a diameter of several hundred micrometers [29].

In this study, we developed a novel patterning technique to control the structure of a multiscale vascular network composed of endothelialized channels with a diameter of several hundred micrometer and microvessels with a diameter of several tens of micrometers. In order to induce sprouting that forms blood vessels of several tens of μm in diameter connected to the blood vessel channel in the engineered tissue, it is important to form concentration gradient of angiogenic factors. Angiogenesis can be induced by adding angiogenic factors to culture media, biomaterials or micro-beads. However, it is not possible to form the gradient by adding to media, and it is not easy to supply sustained angiogenic factors over a long period of time by using biomaterials or microbeads. In this study, we developed a system to continuously supply necessary factors by co-printing with angiogenic factor secreting fibroblasts and endothelial cells.

An endothelialized channel of several hundred micrometers in diameter was fabricated by patterning endothelial cell-laden soluble bio-ink. Using co-printed fibroblasts, a gradient of angiogenic factor was formed along the bridge pattern. Angiogenesis is promoted at lower matrix density[10, 12, 13]. However, a matrix with low density is difficult to maintain a structure for a long time. We used a low concentration of fibrin gel for the production of bridge pattern, and induced angiogenesis through it. And the higher concentration of fibrin gel was used as the surrounding matrix to improve the integrity of the structure. Using the difference in density of the two materials, angiogenic sprouting was induced only in the bridge pattern, thereby successfully forming a designed micro-vascular network with diagonal, wave and branch patterns. These results show that the design of a multiscale vascular network consisting of several hundred micrometers and tens of micrometers tubular blood vessels can be freely controlled.

The micro-vascular network developed in this study did not show sufficient function in terms of in-vitro perfusion. It was observed that the fluorescent micro-beads only partially passed through the vascular network with a diameter of several tens of μm connected to the endothelial channel (Fig. 5f). But, this result means the induced vascular network was well connected to the endothelialized channel. In addition, a confocal microscope confirmed that the induced vascular network has a tubular shape (Fig. 5e). The reason that micro-beads did not pass through micro-vessels completely is considered that the micro-vascular network was not sufficiently matured. In this study, cultivation was performed only in a static environment after printing. Previous studies have shown that dynamic culture conditions with flow have a significant effect on the maturity of blood vessel [30, 31]. Therefore, in future studies, we will perform a research on the improvement of maturity of micro-vascular network by dynamic culture. Using dynamic culture, the problem of micro-beads flow could be solved. On the other hand, Chen et

al. introduced a technique for forming a vascular channel with a parallel pattern using a mold [3]. They produced vascular structures with a scale of several tens of micrometers and successfully demonstrated the flow of blood through the implanted vessels in an animal study. The micro-vascular network derived from our study is very similar to that of the study of Chen et al. when viewed in terms of material composition and form. Based on these findings, we expect that the in vivo function of the multiscale vascular network developed in this study will be show sufficient function.

In this study, the possibility of formation of biomimetic vascular network and its functionality were verified by applying our developed process to liver tissue engineering. A hexagonal structure mimicking the lobule structure of the liver tissue and a structure with a radial micro-vascular network were successfully constructed (Fig. 10g). The effect of the biomimetic vascular network on the function of parenchymal cells was analyzed. As a result, we confirmed that the multiscale vascular network significantly enhanced the albumin and urea secretion of mouse primary hepatocytes (Fig. 10k and l). In particular, urea showed a 40-fold increase over the control group. These results show that it is possible to fabricate biomimetic and multiscale vascular networks specialized in various tissues using the process developed in this study. In addition, it shows the possibility of greatly improving the functionality of a specific cell or tissue using our strategy. The micro-vessels of in vivo tissues have a specific structure for the tissue. The microfluidic environment formed by the vascular structure is directly related to the survival and function of the tissue. The technique developed in this study will provide a very useful tool for artificial regeneration of biomimetic tissue with a multiscale vascular network of complex structure.

5. Conclusion

In conclusion, we developed a technique to control the patterns of in vitro micro-vascular networks using bioprinting, and confirmed the functionality of the artificial liver tissue formed by co-culturing the developed micro-vascular structures and primary hepatocytes. Our technique can be applied not only to liver tissue but also to other kinds of tissues with tissue-specific micro-vascular networks. It can also be used for biological research and medical research, which can contribute to advances in tissue engineering.

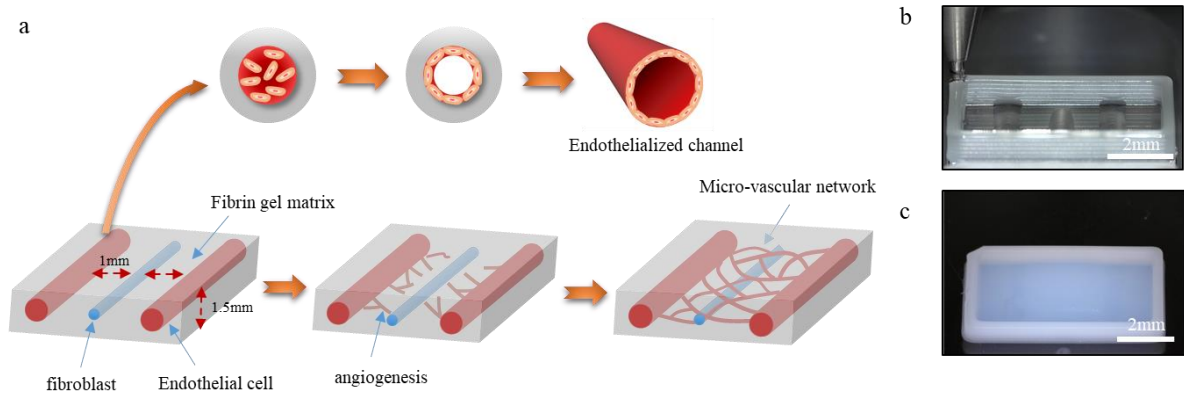


Fig. 1.

Formation of endothelialized channel and micro-vascular network. (a) Schematics of process of endothelialized channel formation and micro-vascular network formation in vascular construct fabricated by 3D bioprinting. (b, c) Optical images of printed structure before (b) and after (c) covering fibrin gel as a surrounding matrix (scale bar, 2mm).

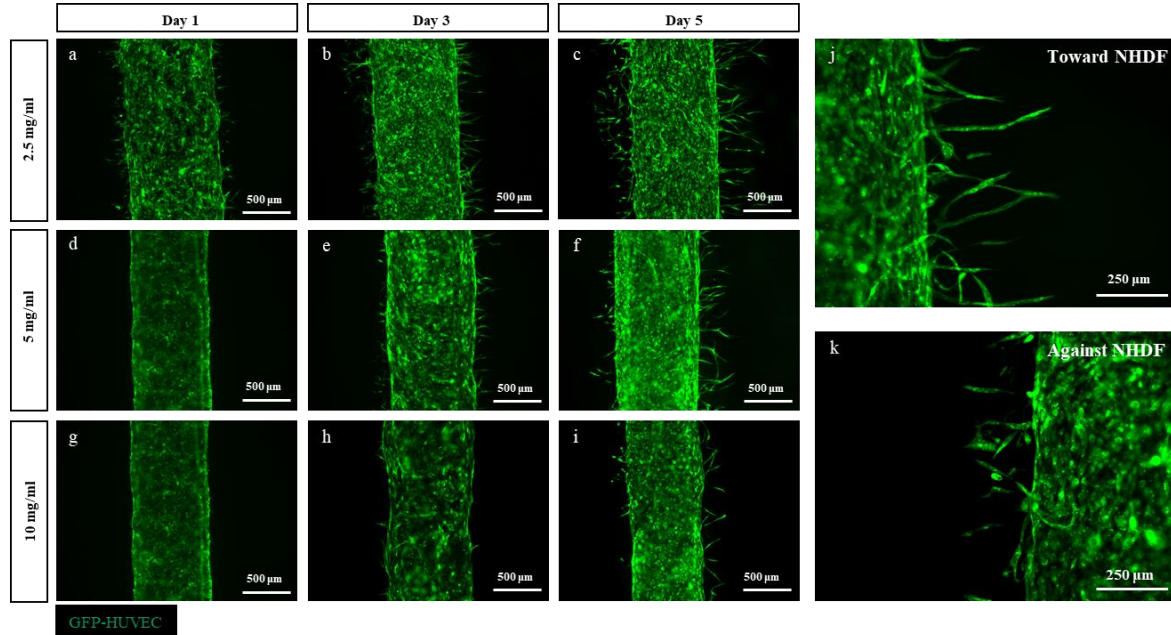


Fig. 2.

Sprouting from HUVEC channel is more active in lower concentration gel; in 2.5 mg/ml (a-c), 5 mg/ml (d-f) and 10 mg/ml fibrin gel (g-i). Sprouts extended more toward NHDF (j) than against NHDF (k).

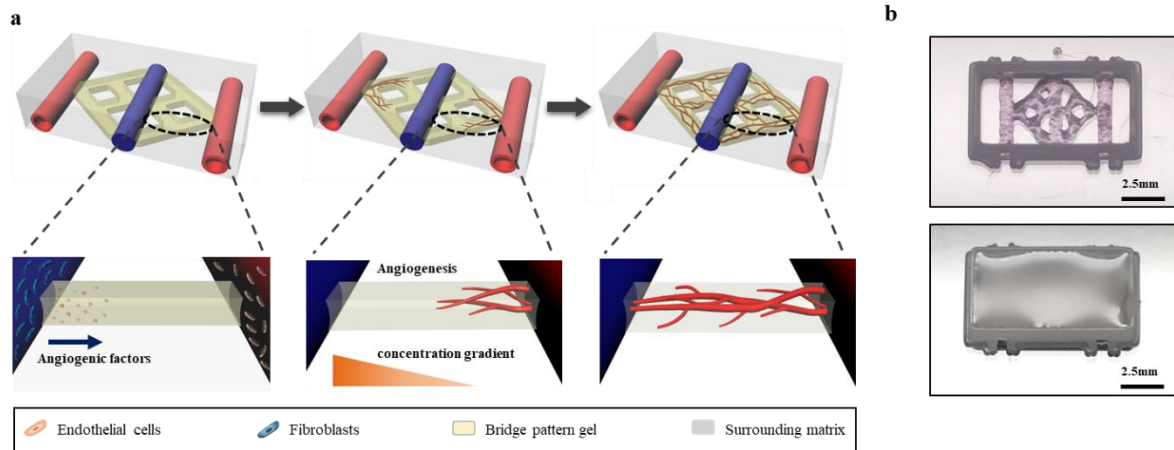


Fig. 3.

3D printed vascular structure to induce designed vascular network. (a) Schematics of process of micro-vascular network patterning. By patterning low concentration fibrin gel (bridge pattern gel) and inducing angiogenesis, micro-vascular network can be patterned. (b, c) Optical images of printed construct before (b) and after (c) fibrin gel covering.

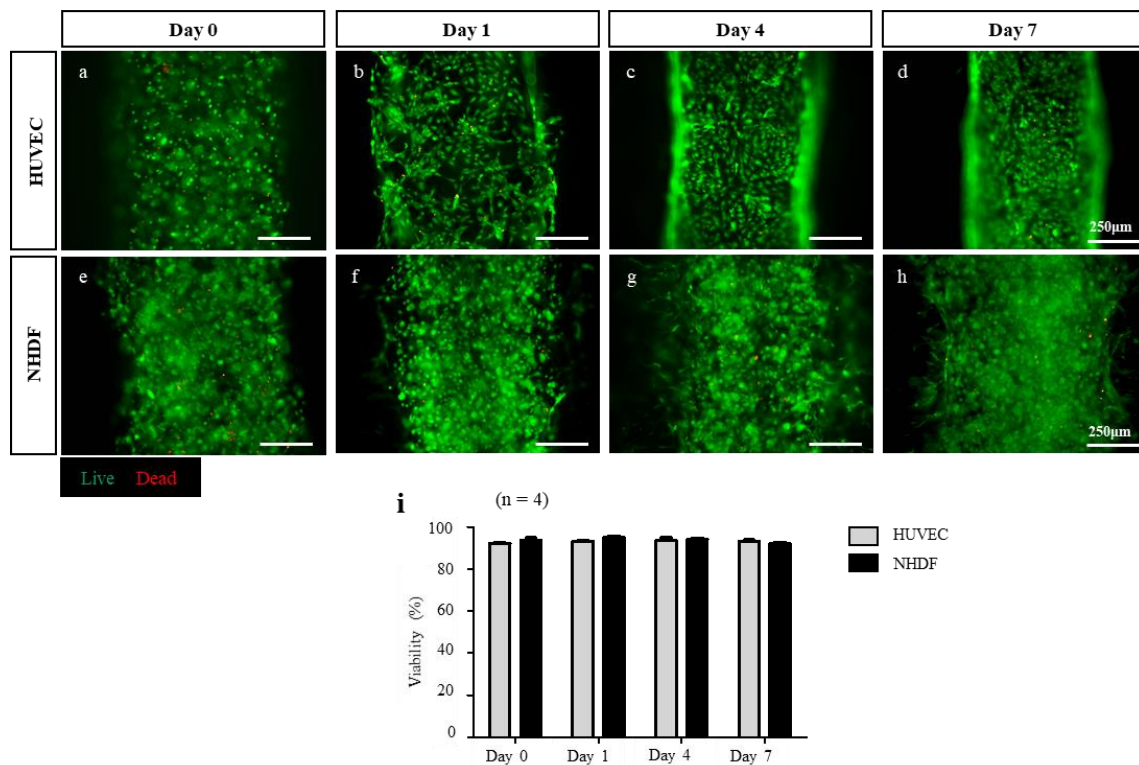


Fig. 4.

Viability assay of printed 3D vascular construct. (a-h) Fluorescence images of HUVEC and NHDF in printed vascular construct labeled with calcein (live) and ethidium homodimer (dead). (i) Cell viability was over 90% on day 0 and then maintained until day 7. Data are expressed as mean \pm s.d. (n = 4 samples per group).

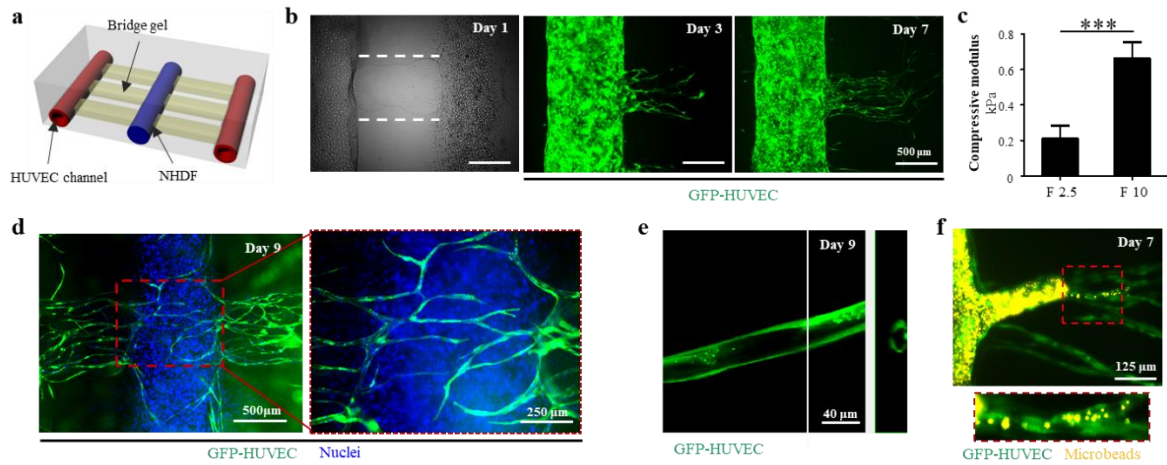


Fig. 5.

Construction of patterned micro-vascular network by bridge gel patterning. (a) Schematic of structure of 3D vascular construct. (b) Sprouting occurred only within bridge pattern and extended over time. (c) The compressive modulus of surrounding matrix (fibrinogen 10 mg/ml) is three times bridge pattern gel (fibrinogen 2.5 mg/ml). Data are expressed as mean \pm s.d. (n = 8 samples per group, ***P < 0.0001). (d) Micro-vessels growing from both HUVEC channels were connected to each other on day 9. (e) Luminal structure of micro-vessel on day 9. (f) When fluorescent beads were injected into the HUVEC channel, the beads partially flowed into the micro-vessel.

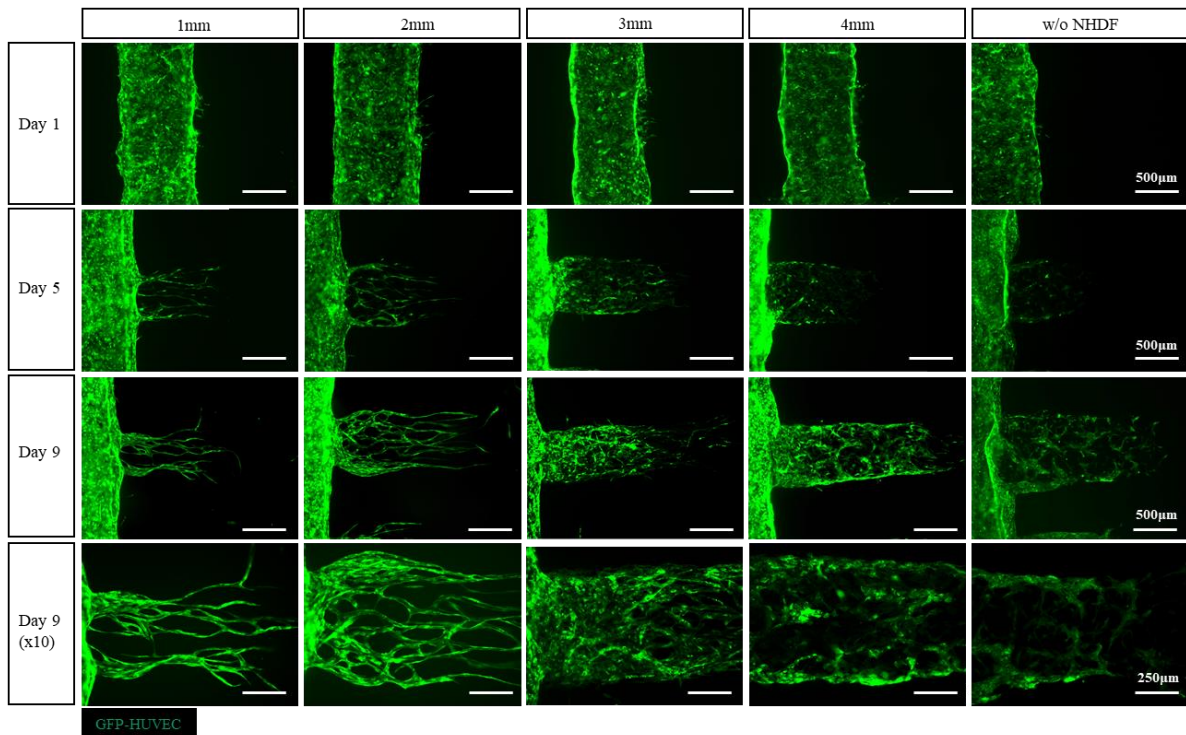


Fig. 6.

Distance between HUVEC channel and NHDF pattern affect micro-vascular network formation. Fluorescence images of angiogenesis process in printed structure with different distance between HUVEC channel and NHDF pattern. In the group of 1 and 2mm groups sprouts was hollow and the junction was well formed and spread out in the bridge pattern. However, in 3 and 4 mm groups, ECs grew in the similar pattern as the control group (without NHDF) without the formation of the vascular network.

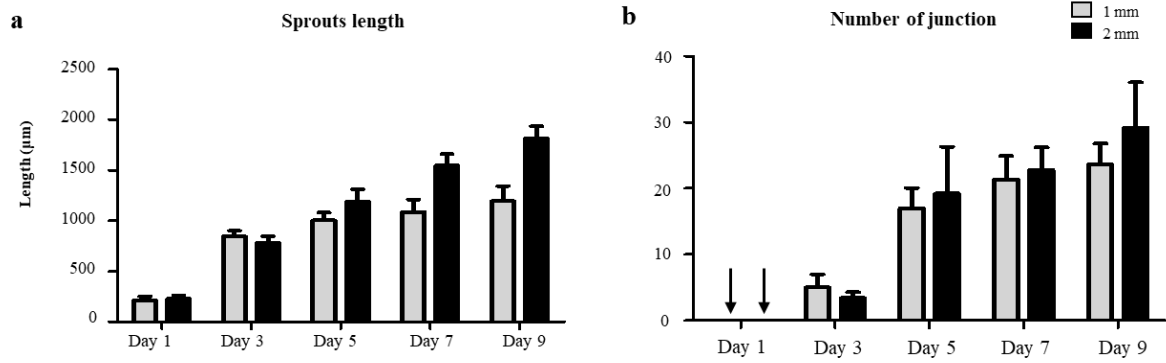


Fig. 7.

Quantification of angiogenic sprouting in 3D vascular construct. (a) Quantification of angiogenic sprout growth by tip cell distance from the edge of HUVEC channel. Data are expressed as mean \pm s.e.m. (n = 5 samples per group, 3 sprouts per sample). (b) Quantification of number of junction of micro-vascular network. Data are expressed as mean \pm s.d. (n = 5 samples per group).

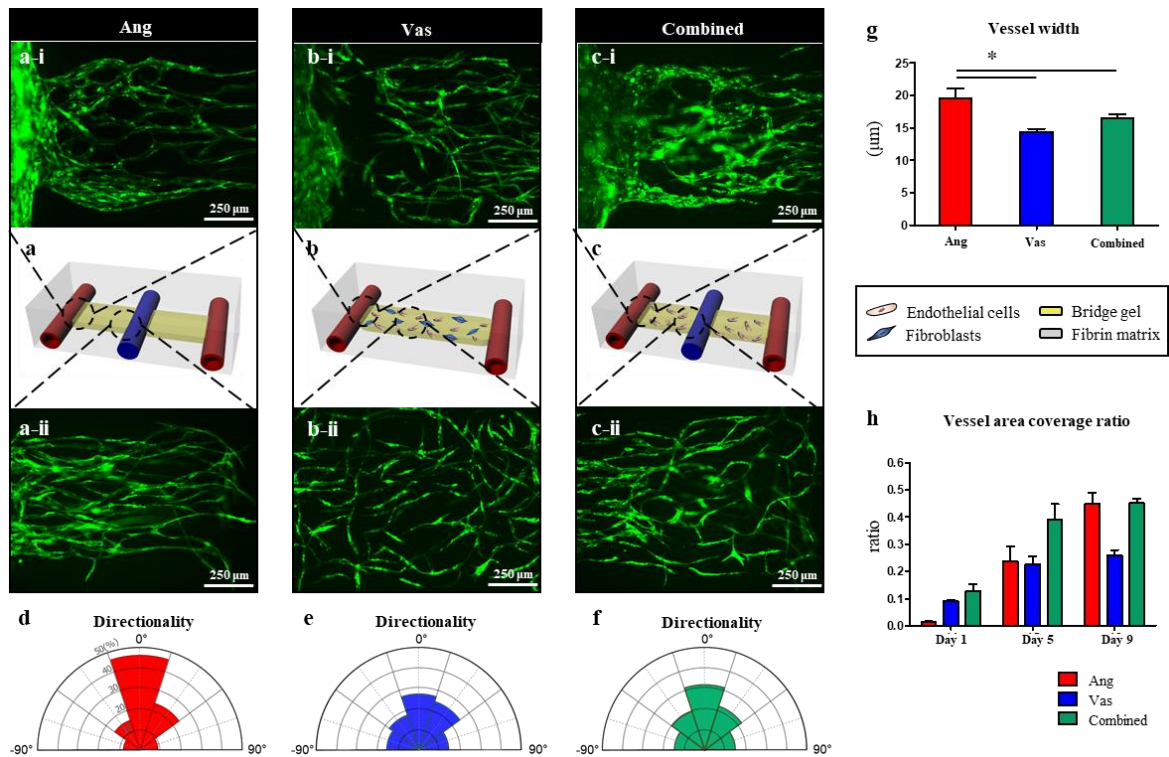


Fig. 8.

Comparison between three groups with different methods to induce micro-vascular network. (a-c) Schematics of angiogenesis model(Ang) (a), vasculogenesis model(Vas) (b) and combined model (c). Fluorescence image of induced micro-vascular network near the HUVEC channel (a-i, b-i, c-i) and the central part of the construct (a-ii, b-ii, c-ii) on day 9. (d-f) Semicircle graphs show the distribution of directionality of micro-vessels in the three groups. 0° represents the vessel is perpendicular to the HUVEC channel. (g) Graph shows vessel width of three groups on day 9. Data are expressed as mean \pm s.e.m. (n = 5 samples per group, 10 micro-vessels per sample, *P<0.05). (h) Graph shows the proportion of vessel area coverage to bridge pattern. Data are expressed as mean \pm s.d. (n = 4 samples per group).

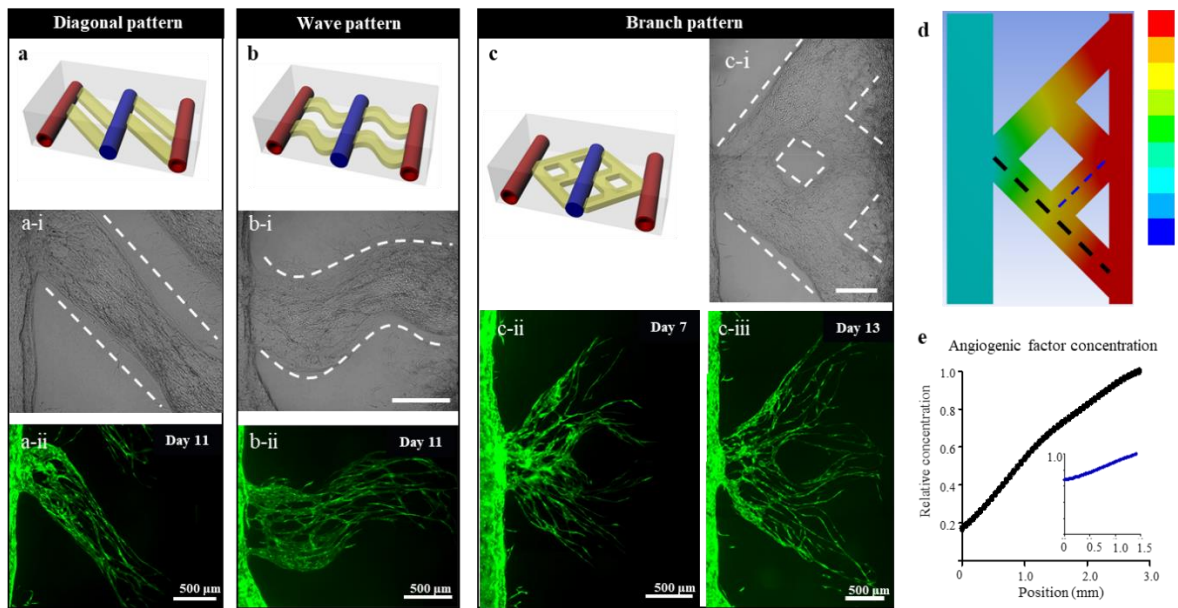


Fig. 9.

Formation of micro-vascular network with various pattern. (a-c) Schematics of the structure having a diagonal, wave and branch pattern (Red: HUVEC-laden gelatin gel, blue: NHDF-laden alginate gel, yellow: bridge pattern). Phase contrast images (a-i, b-i, c-i) and fluorescent images (a-ii, b-ii, c-ii, c-iii) of the patterned micro-vessels in bridge pattern: green, GFP-HUVEC. (d) Simulation of diffusion of angiogenic factors released from NHDF-laden alginate gel to the branch bridge pattern. The image show the molecular diffusion after 24 hours culture. (e) Graphs show relative concentration of angiogenic factors in the bridge pattern. The location of gradient in graphs is indicated by black and blue lines.

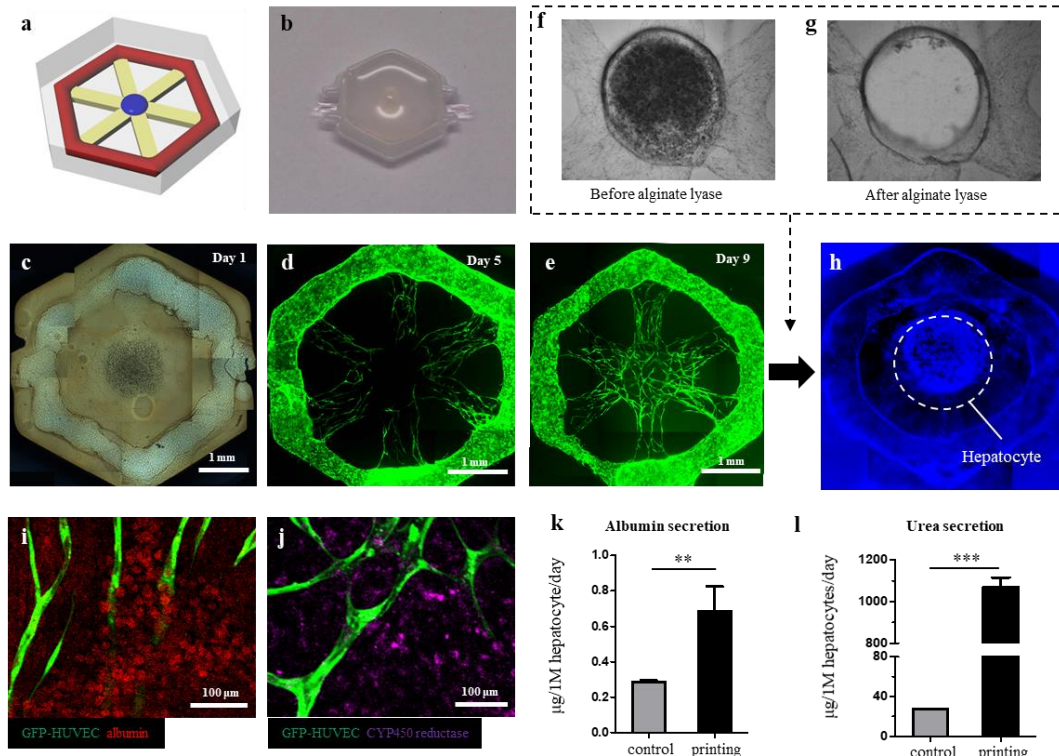


Fig. 10.

Fabrication of bio-mimetic liver lobule structure. (a) Diagram of the liver lobule structure (Red: HUVEC-laden gelatin gel, blue: NHDF-laden alginate gel, yellow: bridge pattern). (b) Optical image of printed liver lobule structure. Microscopic images of alginate gel printed position before (c) and after (d) alginate lyase treatment. Microscopic image (e) and fluorescent images (f, g) of the micro-vessels in printed lobule structure. (h) After alginate lyase treatment, mouse primary hepatocytes were seeded in the position of alginate gel. Immunofluorescence images of micro-vascularized liver lobule tissue of 3 days after cell seeding. Hepatocytes were immunostained with mouse-Albumin (i) and CYP450 reductase antibody (j). (k, l) Quantification of albumin (k) and urea (l) secretion from micro-vascularized liver tissue and 3D fibrin gel control on day 4. Data are expressed as mean \pm s.d. (n = 4 samples per group, **P<0.001, ***P < 0.0001).

References

- [1] M. A. S. K. R. Stevens, V. Ramanan, C. L. Fortin, R. R. Chaturvedi, K. A. Knouse, J.W.Xiao, C.Fung, T.Mirabella,A.X.Chen, M.G. McCue, M. T.Yang, H. E. Fleming, K. Chung, Y. P. de Jong, C. S. Chen, C. M. Rice, S. N. Bhatia, "In situ expansion of engineered human liver tissue in a mouse model of chronic liver disease," *Sci. Transl. Med.* , 2017.
- [2] T. Mirabella *et al.*, "3D-printed vascular networks direct therapeutic angiogenesis in ischaemia," *Nat Biomed Eng*, vol. 1, 2017.
- [3] J. D. Baranski *et al.*, "Geometric control of vascular networks to enhance engineered tissue integration and function," *Proc Natl Acad Sci U S A*, vol. 110, no. 19, pp. 7586-91, May 07 2013.
- [4] J. S. Miller *et al.*, "Rapid casting of patterned vascular networks for perfusable engineered three-dimensional tissues," *Nat Mater*, vol. 11, no. 9, pp. 768-74, Sep 2012.
- [5] L. Zhao, V. K. Lee, S. S. Yoo, G. Dai, and X. Intes, "The integration of 3-D cell printing and mesoscopic fluorescence molecular tomography of vascular constructs within thick hydrogel scaffolds," *Biomaterials*, vol. 33, no. 21, pp. 5325-32, Jul 2012.
- [6] D. B. Kolesky, R. L. Truby, A. S. Gladman, T. A. Busbee, K. A. Homan, and J. A. Lewis, "3D bioprinting of vascularized, heterogeneous cell-laden tissue constructs," *Adv Mater*, vol. 26, no. 19, pp. 3124-30, May 21 2014.
- [7] D. B. Kolesky, K. A. Homan, M. A. Skylar-Scott, and J. A. Lewis, "Three-dimensional bioprinting of thick vascularized tissues," *Proc Natl Acad Sci U S A*, vol. 113, no. 12, pp. 3179-84, Mar 22 2016.
- [8] H. Gerhardt *et al.*, "VEGF guides angiogenic sprouting utilizing endothelial tip cell filopodia," *J Cell Biol*, vol. 161, no. 6, pp. 1163-77, Jun 23 2003.
- [9] R. H. Adams and K. Alitalo, "Molecular regulation of angiogenesis and lymphangiogenesis," *Nat Rev Mol Cell Biol*, vol. 8, no. 6, pp. 464-78, Jun 2007.
- [10] C. M. Ghajar *et al.*, "The effect of matrix density on the regulation of 3-D capillary morphogenesis," *Biophys J*, vol. 94, no. 5, pp. 1930-41, Mar 01 2008.
- [11] A. Blasi *et al.*, "Dermal fibroblasts display similar phenotypic and differentiation capacity to fat-derived mesenchymal stem cells, but differ in anti-inflammatory and angiogenic potential," *Vascular Cell*, journal article vol. 3, no. 1, p. 5, February 08 2011.
- [12] R. R. Rao, A. W. Peterson, J. Ceccarelli, A. J. Putnam, and J. P. Stegemann, "Matrix composition regulates three-dimensional network formation by endothelial cells and mesenchymal stem cells in collagen/fibrin materials," *Angiogenesis*, journal article vol. 15, no. 2, pp. 253-264, June 01 2012.
- [13] E. Kniazeva and A. J. Putnam, "Endothelial cell traction and ECM density influence both

- capillary morphogenesis and maintenance in 3-D," *Am J Physiol Cell Physiol*, vol. 297, no. 1, pp. C179-87, Jul 2009.
- [14] V. K. Lee, A. M. Lanzi, N. Haygan, S. S. Yoo, P. A. Vincent, and G. Dai, "Generation of Multi-Scale Vascular Network System within 3D Hydrogel using 3D Bio-Printing Technology," *Cell Mol Bioeng*, vol. 7, no. 3, pp. 460-472, Sep 2014.
- [15] S. Kim, H. Lee, M. Chung, and N. L. Jeon, "Engineering of functional, perfusable 3D microvascular networks on a chip," *Lab Chip*, vol. 13, no. 8, pp. 1489-1500, Apr 21 2013.
- [16] J. M. Chan, I. K. Zervantonakis, T. Rimchala, W. J. Polacheck, J. Whisler, and R. D. Kamm, "Engineering of in vitro 3D capillary beds by self-directed angiogenic sprouting," *PLoS One*, vol. 7, no. 12, p. e50582, 2012.
- [17] T. Osaki, T. Kakegawa, T. Kageyama, J. Enomoto, T. Nittami, and J. Fukuda, "Acceleration of vascular sprouting from fabricated perfusable vascular-like structures," *PLoS One*, vol. 10, no. 4, p. e0123735, 2015.
- [18] K. Sasaki *et al.*, "Construction of three-dimensional vascularized functional human liver tissue using a layer-by-layer cell coating technique," *Biomaterials*, 2017.
- [19] H. Sekine *et al.*, "In vitro fabrication of functional three-dimensional tissues with perfusable blood vessels," *Nat Commun*, vol. 4, p. 1399, 2013.
- [20] J. H. Kang, J. M. Gimble, and D. L. Kaplan, "In vitro 3D model for human vascularized adipose tissue," *Tissue Eng Part A*, vol. 15, no. 8, pp. 2227-36, Aug 2009.
- [21] K. T. Morin, A. O. Smith, G. E. Davis, and R. T. Tranquillo, "Aligned human microvessels formed in 3D fibrin gel by constraint of gel contraction," *Microvasc Res*, vol. 90, pp. 12-22, Nov 2013.
- [22] J. D. Baranski *et al.*, "Geometric control of vascular networks to enhance engineered tissue integration and function," *Proceedings of the National Academy of Sciences*, vol. 110, no. 19, pp. 7586-7591, 2013.
- [23] K. R. Stevens *et al.*, "In situ expansion of engineered human liver tissue in a mouse model of chronic liver disease," *Science translational medicine*, vol. 9, no. 399, p. eaah5505, 2017.
- [24] T. Mirabella *et al.*, "3D-printed vascular networks direct therapeutic angiogenesis in ischaemia," *Nature Biomedical Engineering*, vol. 1, no. 6, p. 0083, 2017.
- [25] J. S. Miller *et al.*, "Rapid casting of patterned vascular networks for perfusable engineered three-dimensional tissues," *Nature materials*, vol. 11, no. 9, p. 768, 2012.
- [26] L. Zhao, V. K. Lee, S.-S. Yoo, G. Dai, and X. Intes, "The integration of 3-D cell printing and mesoscopic fluorescence molecular tomography of vascular constructs within thick hydrogel scaffolds," *Biomaterials*, vol. 33, no. 21, pp. 5325-5332, 2012.
- [27] D. B. Kolesky, K. A. Homan, M. A. Skylar-Scott, and J. A. Lewis, "Three-dimensional bioprinting of thick vascularized tissues," *Proceedings of the National Academy of Sciences*,

- vol. 113, no. 12, pp. 3179-3184, 2016.
- [28] D. B. Kolesky, R. L. Truby, A. S. Gladman, T. A. Busbee, K. A. Homan, and J. A. Lewis, "3D bioprinting of vascularized, heterogeneous cell-laden tissue constructs," *Advanced materials*, vol. 26, no. 19, pp. 3124-3130, 2014.
- [29] V. Malkoc, "Challenges and the future of 3D bioprinting," *J Biomed*, vol. 1, no. 3, p. 62, 2018.
- [30] A. Lenard *et al.*, "In vivo analysis reveals a highly stereotypic morphogenetic pathway of vascular anastomosis," *Dev Cell*, vol. 25, no. 5, pp. 492-506, Jun 10 2013.
- [31] E. A. Jones, F. le Noble, and A. Eichmann, "What determines blood vessel structure? Genetic prespecification vs. hemodynamics," *Physiology (Bethesda)*, vol. 21, pp. 388-95, Dec 2006.

